Colloid Polym Sci 276:412–419 (1998)
© Steinkopff Verlag 1998

ORIGINAL CONTRIBUTION

S. Shimada
K. Horiguchi
K. Yamamoto

Structure and molecular motion of poly(ethylene oxide) chains adsorbed on a silica-tethered poly(methyl methacrylate) by the spin label method

Received: 4 September 1997
Accepted: 9 December 1997

Dr. S. Shimada (✉) · K. Horiguchi
K. Yamamoto
Nagoya Institute of Technology
Gokiso-cho, Showa-ku
Nagoya 466
Japan

Abstract The spin-label method was used to study the structure and molecular motion of poly(ethylene oxide) (PEO) chains adsorbed on a silica-tethered poly(methyl methacrylate) (PMMA). Spin-labelled PEO with a narrow molecular weight distribution, having number averaged molecular weight (M_N) $= 6.0 \times 10^3$, was adsorbed on the surface of the silica-tethered PMMA with various grafting ratios in carbon tetrachloride solution at 35 °C. ESR spectra were measured at various temperatures after the samples were completely dried.

The ESR spectra are composed of two spectra arising from spin-labels attached to "train" and "tail" segments, which are strongly and weakly interacted with the silica surface, respectively. The fractional amount of the "tail" segments increases extremely with the grafting ratio of PMMA. Molecular mobility of the PEO chains estimated from the temperature dependence of the ESR spectra also decreases significantly with the grafting ratio of PMMA.

Structure and molecular motion of the PMMA chains tethered on the silica were also studied using the spin-labelled PMMA.

Consequently, parts of the PEO segments penetrate into the PMMA chains and is adsorbed on the silica surface ("train" segments), whereas parts of the PMMA segments protrude from the surface. The other PEO segments are entangled with the tethered PMMA chains ("tail" segments).

Key words poly(ethylene oxide) – silica-tethered poly(methyl methacrylate) – adsorption – spin-label – molecular motion

Introduction

Many investigations by ESR method have been published concerning adsorption of polymer on the silica surface [1–6]. Kawaguchi and coworkers [7, 8] studied the adsorption behaviors of poly(ethylene oxide) (PEO) and the competitive displacement and adsorption of polystyrene (PS) and PEO on a nonporous silica. They concluded that PEO molecules were strongly attached to the silica surface via hydrogen bonding between surface silanol group and the oxygen atom in the etoxy segment of PEO.

In our previous papers [9, 10] the spin label method was used to study the structure and molecular motion of PS chains adsorbed on a silica tethered PEO in comparison with those of the tethered PEO. It was concluded that the large PS molecules penetrated into the PEO chains and were adsorbed on the surface as "train" segments, whereas the small PS molecules were entangled with the PEO chains. The interesting molecular weight dependence of the adsorption behavior suggests that in spite of the immiscibility of PS with PEO, the PS molecules have different interactions with the tethered PEO molecules compared to the interactions between PS and PEO molecules in the homopolymer blend. It is well known that PEO is miscible with atactic poly(methyl methacrylate) (PMMA). At present, we are interested in the effect of the tethered PMMA on the adsorption behavior of the PEO chains and structure and molecular motion of the PEO chains on the silica-tethered PMMA. The tethered PMMA segments may be weakly adsorbed because of their bulkiness, and the high miscibility of PEO with PMMA may give rise to a unique adsorption behavior unlike that in the system of PEO/PS.

In this paper, we report the adsorption behavior of PEO, each structure and molecular motion of the PEO and the tethered PMMA chains.

Experimental

Materials

A poly(ethylene oxide) having number average molecular weight (M_N) = 6.0×10^3 (PEO-6) was purchased from Katayama Science Co. (Tokyo, Japan). The polydispersity of PEO-6 was < 1.20. The PEO-6 was purified by precipitating from chloroform solution by addition of diethylether and dried under vacuum for more than 1 d at room temperature. Ends of the PEO chains were spin-labelled by the method of Törmälä et al. [11].

The nonporous silica particles used for the adsorbent were micro bead (70–230 mesh) silica gels purchased from Nacalai Tesque Co. (Tokyo, Japan). The surface area of the silica gels was 376 m^2/g.

Grafting reaction

Methyl methacrylate (MMA) monomer was purified by distillation. MMA, benzene, initiator (benzoyl peroxide) and silica gels were put into a reaction vessel. The solution containing the silica gels was purged using nitrogen gas at $70 \pm 0.5\,^{\circ}C$. The grafting ratio increases with an increase in reaction time. In order to compare adsorption behaviors of PEO on a silica tethered PMMA with those on a silica tethered PS, styrene monomer was also graft-polymerized on the silica gel by the same method. A small amount of labelled monomer, 4-(methacryloyloxy)-2,2,6,6-tetra methyl piperidine-1-oxyl was added with the other reagents and the silica gels in order to obtain the tethered and spin-labelled PMMA sample [12–14].

After the grafting reaction was achieved, the PMMA homopolymer was removed by extraction with acetone in a Soxhlet for 60 h. The grafted silica was dried under vacuum at 130 °C for 1 day. The grafting ratio (weight ratio of PMMA to silica) was determined by pyrolysis weight loss between 300 and 450 °C. TG (thermogravimetry) measurements were carried out using a Rigaku-TG 8110D calorimeter. TG scans were run from 20 °C to 600 °C at 5 °C/min.

Adsorption of poly(ethylene oxide)

Silica-tethered PMMA (0.2 g) was transferred to a 20 ml flask containing 3 ml of CCl_4. Next, SL-PEO (0.015 g) was dissolved in 4 ml of CCl_4. The polymer solution was transferred to the 20 ml flask containing the mixture of CCl_4 and silica gels. The polymer solution and the mixture in the flask were shaken to attain equilibrium at 100 rpm in a Yamato BT-23 water incubator attached with a shaker. For all experiments, the temperature of the water incubator was controlled to $35.0 \pm 0.1\,^{\circ}C$. The concentration of the polymer solution, 2.1×10^{-3} g/ml does not exceed a critical entanglement concentration [6]. After the adsorption experiment was terminated, the supernatant was carefully removed and dried in a vacuum oven at 40 °C for several days.

ESR measurements

ESR measurements were carried out with a JEOL FE3XG and a JEOL ME3XG spectrometer and connected PC9801 computers.

Results and discussion

Absorption of poly(ethylene oxide) on a silica-tethered poly(methyl methacrylate)

In order to study adsorption behaviors of PEO on a silica-tethered PMMA (silica-t-PMMA), the intensity of the ESR spectrum of nitroxide spin labels in the CCl_4 solution was determined. Figure 1 shows plots of the concentration of SL-PEO in the supernatant relative to the concentration before the adsorption as a function of adsorption time. The decreasing of the intensity with an increase in adsorption time should be caused by transfer of PEO molecules in the solution to the silica gels. It was found that PEO molecules were rapidly adsorbed on the silica-t-PMMA, though the adsorption rate is lower than that on non-grafted silica. For example, all PEO segments in the

CCl_4 solution were adsorbed on the silica-t-PMMA having the grafting ratio (GR) of 17% for approximately 100 min. On the other hand, the adsorption rate of PEO molecules on the silica-tethered PS was extremely low and the adsorbed amount was small as indicated in Fig. 1. Only 70% of PEO molecules in the CCl_4 solution were adsorbed on the silica-tethered PS having the lower GR of 4% for 180 min. This different behavior is caused by the different miscibility of PEO with PMMA from that with PS. PEO molecules can penetrate into the tethered PMMA phase easily and a part of the PEO segments can be adsorbed on the silica surface because of the miscibility of PEO with PMMA. On the other hand, the tethered PS chains interrupt the PEO chains more severely from being adsorbed on the silica surface because of the low miscibility.

Fig. 1 The relative concentration of PEO spin labels in the supernatant as a function of adsorption time for silica-t-PMMA having GR = 17% (○), silica-tethered PS having GR = 4% (●), and non-grafted silica (▲)

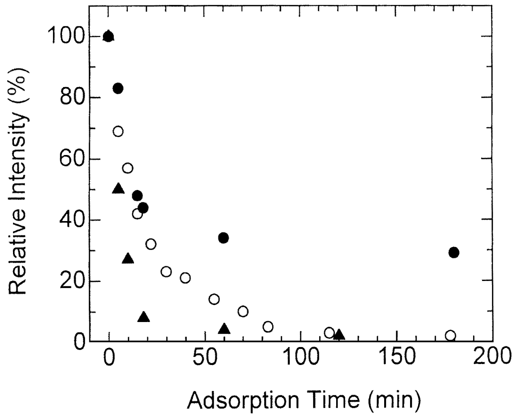

Structure of PEO chains adsorbed on a silica-tethered PMMA

We clarify the structure of PEO chains adsorbed on a silica-t-PMMA surface by using two-component analysis of ESR spectra of spin-labelled PEO (SL-PEO). In order to obtain the exact parameters and clarify the structures of the adsorbed PEO segments, spectral simulations for the ESR spectra are performed [5]. Figure 2 shows an example of the experimental and calculated spectra of SL-PEO on the surface of silica-t-PMMA having the grafting ratio of 13%. The outermost peaks in the high and low magnetic field appear like plateaus in the ESR spectrum. The flat peaks suggest that two-component analysis is reasonable for the ESR spectrum. The simulated spectrum (dotted line in Fig. 2a) by assuming two components (dotted lines in Fig. 2b) shows a good agreement with the observed spectrum (solid line in Fig. 2a). This result indicates the classification of the spin-labels (A-labels and B-labels having high and low values of hyperfine splitting (hfs)) affected by different environments is a good approximation as discussed previously [5, 6]. The ESR parameters determined from the spectral simulation are shown in Table 1.

The variation of *A* value in the table should arise from the electric field of the polar group as concluded by

Fig. 2 (a) Comparisons of observed (solid) and calculated (dotted) ESR spectra of spin-labelled PEO adsorbed on silica-t-PMMA having the grafting ratio of 13%. The measurement was carried out at 203 K. The calculated spectrum (a) is composed of two spectra (b)

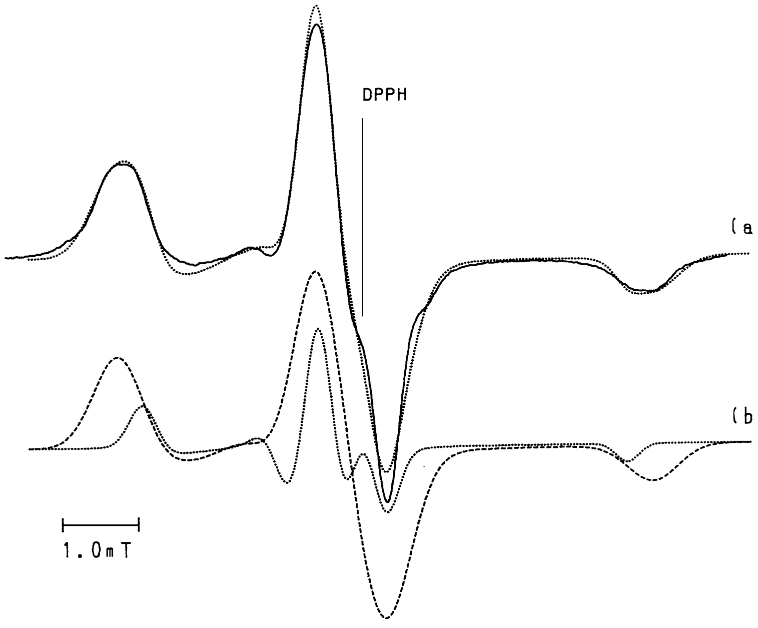

Table 1 ESR parameters of spectra of SL-PEO adsorbed on the silica-t-PMMA having the grafting ratio of 13%, determined from the simulation spectrum mentioned in the text. The ESR measurement was carried out at 203 K. Those of SL-PEO in the homopolymer bulk observed at 77 K are also indicated

ESR parameters	Silica-t-PMMA + SL-PEO		SL-PEO/bulk
	A	B	
g_Z	2.0016	2.0017	2.0021
g_Y	2.0056	2.0060	2.0065
g_X	2.0078	2.0072	2.0080
$\frac{1}{3}(g_X + g_Y + g_Z)$	2.0050	2.0050	2.0055
A_Z (mT)	3.50	3.18	3.30
A_Y (mT)	0.48	0.55	0.43
A_X (mT)	0.48	0.55	0.43
$\frac{1}{3}(A_X + A_Y + A_Z)$	1.48	1.43	1.39
Line width (mT)	0.64	0.31	0.83
Fraction (%)	88	12	100

Griffith et al. [15]. The solvent dependence of ESR spectra can be visualized as arising from changes in the relative contribution of the two valence structures, (a) and (b), of the neutral free radicals:

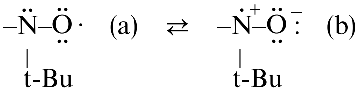
$$\underset{\text{t-Bu}}{-\ddot{\underset{..}{\text{N}}}}-\underset{..}{\ddot{\text{O}}}\cdot \quad \text{(a)} \quad \rightleftarrows \quad \underset{\text{t-Bu}}{-\overset{\cdot +}{\text{N}}}-\underset{..}{\ddot{\text{O}}}\overset{-}{:} \quad \text{(b)}$$

The changes are caused by the electric field of the silica gel surface. Structure (a) localizes it on the oxygen atom, whereas structure (b) localizes it on the nitrogen atom, and the electric field that tends to stabilize (b) is responsible for the increased splitting due to the nitrogen nucleus. A spectrum with high A_Z and A_i values in comparison with those in the homopolymer PEO, reflects a strong PEO–silica interaction (A-labels) and another spectrum with low A_Z and A_i values, reflects a weak PEO–silica interaction (B-labels). The B-labels have the smaller value of A_Z and the larger A_X and A_Y. The partial averaging of A values also suggests that the molecular motion of the segments, weakly interacted with silica, have already occurred. It can be considered that A- and B-labels reflect "train" and "tail" segments, respectively, as shown in Fig. 3.

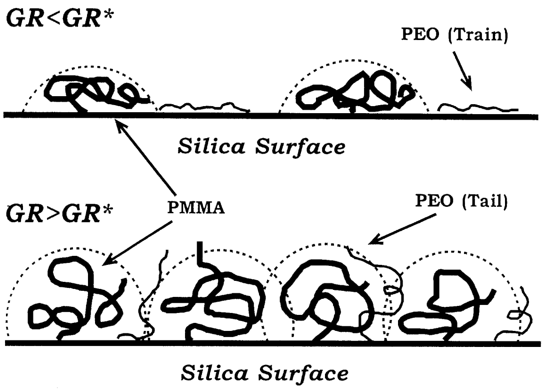

Fig. 3 Schematic representation of structures of PMMA segments on the silica-t-PMMA and the adsorbed segments. The meaning of GR* is mentioned in the text

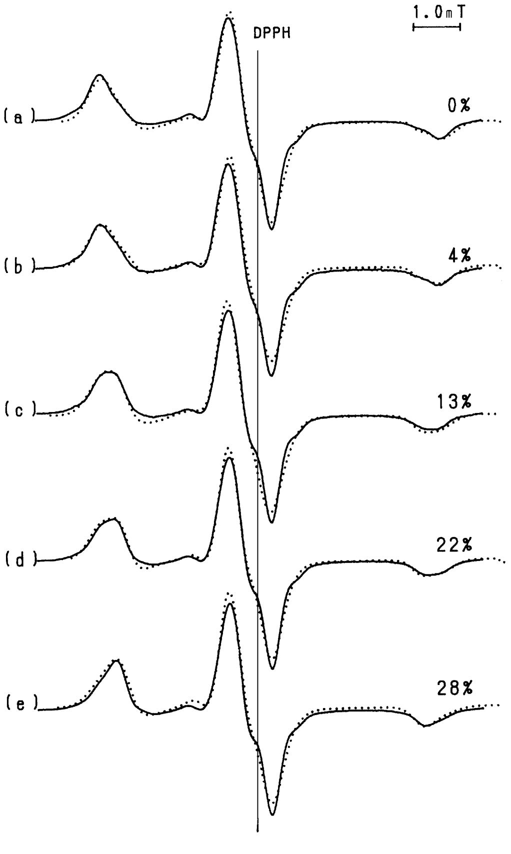

Fig. 4 Variation of ESR spectra of spin-labelled PEO adsorbed on silica-t-PMMA with the grafting ratio. Solid and dotted lines indicate observed and calculated spectra, respectively. The measurement was carried out at 203 K

Figure 4 shows the dependence of ESR spectrum of SL-PEO adsorbed on the silica-t-PMMA on GR. It should be noted that the shapes of the outermost peaks vary remarkably with GR. The simulated spectra show good agreement with the observed spectra. From the spectral simulation, it was found that the dependence of the ESR spectrum was caused by the variation of the fractional amount of B-labels with GR. Figure 5 shows the plots of the fractional amount at 203 K vs. GR. The fractional amount of B-labels increases gradually and begins to increase steeply around 13% with an increase in GR. This result suggests two different adsorption behaviors below and above the crossover grafting ratio, GR*. PEO chains are adsorbed selectively on the silica surface

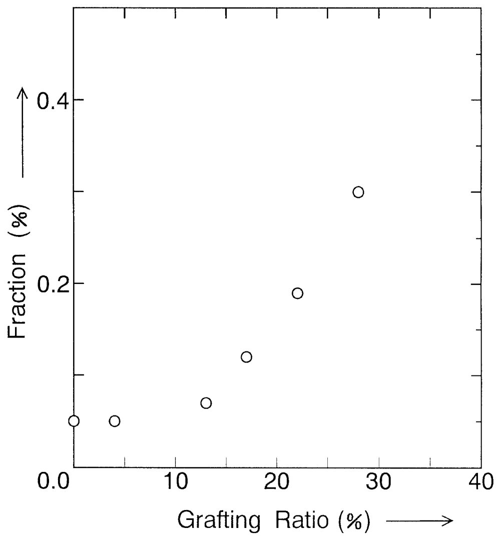

Fig. 5 Fractional amount of B-labels (%) of PEO at 203 K as a function of grafting ratio

which is not occupied by tethered PMMA chains and adopt a flat conformation ("train") at low GR < GR*. On the other hand, at GR > GR*, the tethered PMMA chains begin to interrupt PEO chains from moving to the silica surface and take a "train" conformation. The PEO chains are adsorbed indirectly on the silica, entangling with the PMMA chains because the PMMA chains start to overlap and protrude from the silica surface. Then, the fractional amount of B-labels attached to the "tail" segment increases steeply.

It can be considered that a tethered PMMA chain occupies roughly an hemisphere with a radius comparable to the Flory radius because of its bulkiness on the silica surface. According to an occupied area of an hemisphere of a tethered PEO of the Flory radius evaluated by Hommel et al. [16], 0.15 g of PEO covers the whole surface, 376 m^2 of the silica gel, 1 g. Consequently, the tethered PMMA chains on the silica having GR* = 13% cover approximately the whole surface of the silica when the PMMA chains have the same molecular density as the PEO chains of the Flory radius on the surface. At GR = GR* (ca 13%) the tethered PMMA chains begin to interrupt all PEO segments from being adsorbed on the silica surface, directly.

Molecular motion of PEO chains adsorbed on a silica-tethered PMMA

In order to evaluate the molecular motion of adsorbed PEO chains related to the PEO-silica interactions, ESR spectra were observed at various temperatures. Figure 6 shows temperature dependence of the ESR spectra of SL-PEO adsorbed on the silica(a) and the silica-t-PMMA having GR = 17%(b). Multi-component spectra which are not remarkable for the homopolymer bulk are observed in the wide temperature range. The outermost splitting ($2A_{Z'}$) for both A- and B-labels narrows with increasing motional averaging of the anisotropy of the hyperfine splitting due to the nitrogen nucleus. Spectral components ("s" and "f") of large and small $2A_{Z'}$ values reflect immobile and mobile labels, respectively. For instance, the A-labels convert from the immobile labels to mobile labels with conformational change of "train" chain to "tail" chain above temperatures where a micro Brownian type molecular motion occurs. On the other hand, the B-labels which take a "tail" conformation (are entangled with the PMMA chains) and have a low molecular mobility at low temperatures also convert to the mobile labels when the micro Brownian type molecular motion starts. The spectra of the narrow line width caused by rapid molecular motion appear at extremely low temperatures in comparison with that in the homopolymer PEO bulk. These facts suggest that the PEO chains have a very broad distribution of correlation time of molecular motion caused by the broad distribution of their adsorbed structure. For example, the spectrum of the narrow line width at 293 K is assigned to the end labels of the "tail" segments which move rapidly for the sample of GR = 0% (Fig. 6a) because of low segmental density. The high mobility is caused by the large free space around the PEO chains because of their isolation from the other chains [17–19]. The line width of the narrow component for GR = 17% (Fig. 6b) is larger than that for GR = 0% (Fig. 6a). This experimental fact reflects the increase in the segmental density of PEO and PMMA with an increase in grafting ratio. The fractional amounts of spectrum of larger hfs value for GR = 0% are larger than those for GR = 17% in the whole temperature range. For example, a part of the segments is still strongly interacted with the silica surface at 373 K for GR = 0%, but all PEO segments for GR = 17% move rapidly at the same temperature. The outermost splittings ($2A_{Z'}$) for the SL-PEO on the silica are plotted against temperature in Fig. 7. The value of $2A_{Z'}$ is a good measure of the mobility of the SL-PEO. The width narrowed with an increase in temperature because of averaging of the anisotropic g and hfs values. Both values of $2A_{Z'}$ for the mobile and immobile labels are plotted at higher temperatures above 293 K. The temperature dependence of $2A_{Z'}$ shows a remarkable change with the grafting ratio. The values of $2A_{Z'}$ for the immobile labels are large in the whole temperature range and the immobile labels are alive at high temperatures for the SL-PEO on the non-grafted silica and the silica-t-PMMA having 4% of grafting ratio. The values of $2A_{Z'}$ for the immobile labels

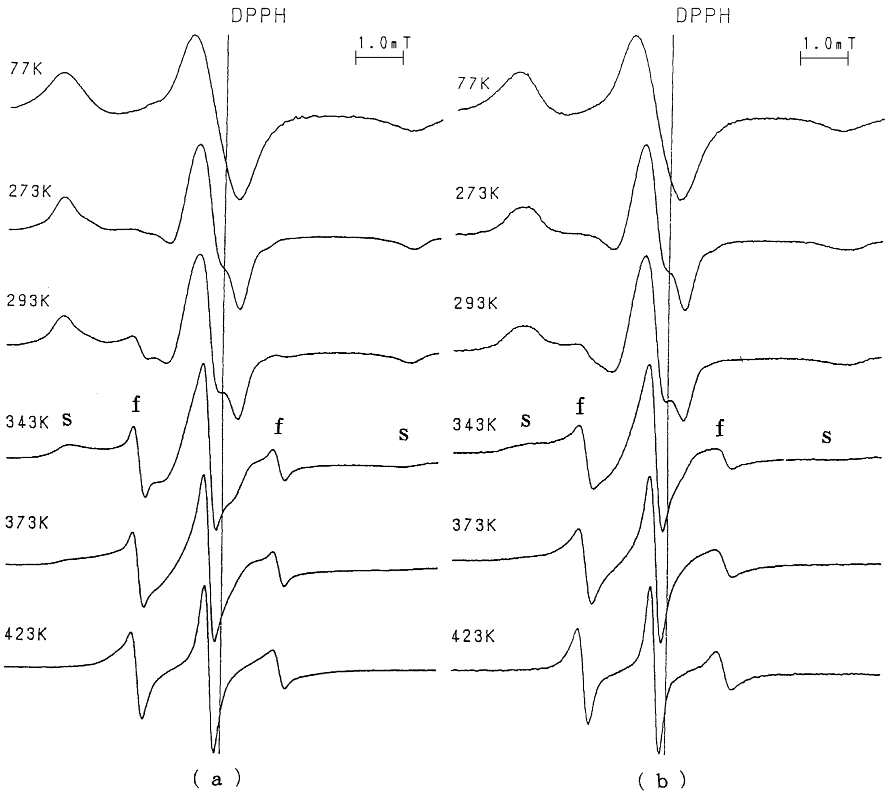

Fig. 6 Temperature dependent ESR spectra of SL-PEO adsorbed on the silica (a) and silica-tethered PMMA having 17% grafting ratio (b). Slow (immobile) and fast (mobile) components are indicated by "s" and "f", respectively

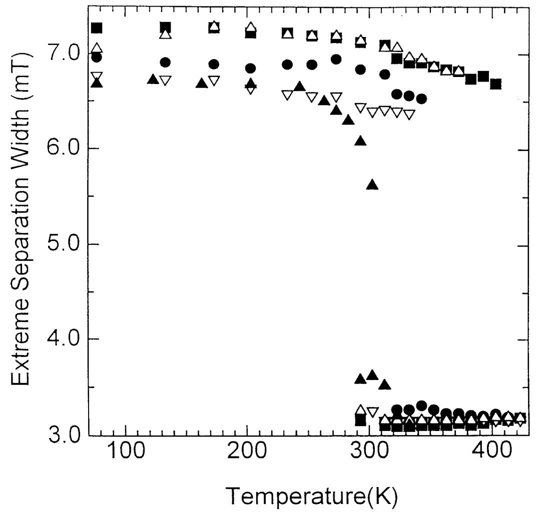

Fig. 7 Variations of outermost splitting ($2A_{Z'}$) with temperature for SL-PEO in solid bulk (▲) and adsorbed on the silica-t-PMMA having the grafting ratios: 0% (■); 4% (△); 13% (●); 28% (▽)

decrease and the temperature where the components disappear decreases with an increase in grafting ratio.

From these experimental facts, the following conclusions can be drawn:

1. Very strong PEO–silica interaction causes a hindrance to the mobility associated with the relaxation of the PEO chains.
2. The mobile PEO segments are protruded from the silica surface and/or entangled with the tethered PMMA chains as concluded in the previous section. Molecular mobility of the PEO chains in the PMMA matrices is lower than that in the PEO matrices since the glass transition temperature (T_g) of PEO (−65 °C) is lower than that of PMMA (108 °C). The tethered PMMA chains slow down the rate of molecular motion of the PEO chains in the homopolymer bulk. Consequently, the transition temperatures for the adsorbed PEO are higher than that for the homopolymer PEO bulk, though the temperatures decrease with an increase in grafting ratio.

Structure and molecular motion of PMMA chains tethered on the silica

Figure 8a shows ESR spectra of SL-PMMA tethered on the silica-t-PMMA having GR = 39%, observed at 77 K. The outermost splitting ($2A_{Z'}$) is larger than for SL-PMMA in the homopolymer PMMA bulk. The high value is also caused by the electric field of the silica surface. In order to obtain the exact ESR parameters, spectral simulations

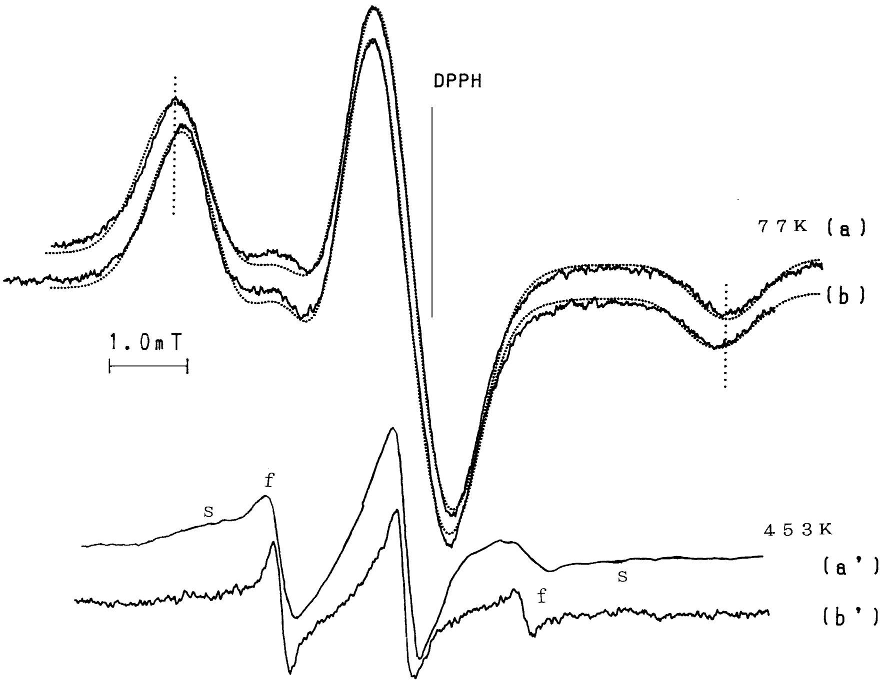

Fig. 8 ESR spectra of spin-labelled PMMA adsorbed on the silica surface having the grafting ratio of 39% before (a), (a′) and (b), (b′) the adsorption of PEO. The measurement was carried out at 77 K (a), (b) and 453 K (a′), (b′). Simulated (dotted) spectra for the spectra observed at 77 K are indicated

for the ESR spectra are performed. The spectra can be also interpreted in terms of two components from two kinds of labels, A- and B-labels. The simulated spectra show good agreement with the observed spectra as indicated in Fig. 8. The ESR parameters determined from the spectral simulations are shown in Table 2. The high values of A_Z (3.61 mT) and A_i $(= A_X + A_Y + A_Z)/3$ (1.63 mT) are caused by the strong electric field of the silica surface. For instance, the PMMA segments connected with the SL-PMMA strongly interacted with the silica as "train" segments. On the other hand, the values of A_Z (3.24 mT) and A_i (1.52 mT) for the tethered PMMA are nearly the same as those of SL-PMMA in the homopolymer PMMA. This is a reflection of the weak interaction of the tethered PMMA segments with the silica. The fractional amount of B-labels, 0.28 is large in comparison with that (0.00) for the adsorbed SL-PEO on the silica at 77 K. The experimental fact is caused by the different bulkiness of PMMA chains from PEO chains. Figure 8b shows the ESR spectrum of SL-PMMA at 77 K after the adsorption of PEO molecules. The outermost splitting after the adsorption is small in comparison with that before adsorption. From the simulation, it is found that the fractional amount of B-labels increases from 0.28 to 0.49 by the adsorption. This fact suggests that a part of the PEO chains penetrate into the tethered PMMA chains and is adsorbed near the silica surface like as "train" segments, whereas a part of the PMMA chains protrude from the silica surface as "loop" or "tail" segments. For instance, the conversion of "train" segments to "loop" or "tail" segments occurs partially on the silica surface. The same experimental results for the silica-t-PMMA have the low grafting ratios of 1.9% and 2.5%. Figure 8a′ and b′ show the ESR spectra of SL-PMMA tethered on the silica-t-PMMA having GR = 39% at 453 K before (a′) and after (b′) the adsorption. The line width of the narrow component before the adsorption of the PEO chains is larger than that after the

Table 2 ESR parameters of spectra of spin-labelled PMMA tethered on the silica having the grafting ratio of 39% before the adsorption of PEO, determined from the simulation spectrum mentioned in the text. Those of SL-PMMA in the homopolymer bulk are also indicated. The ESR measurements were carried out at 77 K

ESR parameters	Silica-t-SL-PMMA		SL-PMMA/bulk
	A	B	
g_Z	2.0021	2.0023	2.0020
g_Y	2.0055	2.0079	2.0064
g_X	2.0094	2.0079	2.0096
$\frac{1}{3}(g_X + g_Y + g_Z)$	2.0057	2.0060	2.0060
A_Z (mT)	3.61	3.24	3.39
A_Y (mT)	0.64	0.67	0.65
A_X (mT)	0.64	0.67	0.65
$\frac{1}{3}(A_X + A_Y + A_Z)$	1.63	1.52	1.56
Line width (mT)	0.80	0.74	0.71
Fraction (%)	72	28	100

adsorption. The fractional amounts of the spectrum of larger hfs value before the adsorption are larger than those after the adsorption. For example, a part of the PMMA segments still have low molecular mobility at 453 K before the adsorption (Fig. 8a′), but all tethered PMMA chains move rapidly at the same temperature after the adsorption (Fig. 8b′). These facts suggest that the PEO molecules give rise to the conformational change of a part of PMMA segments from the “train” segments to the “loop” or “tail” segments and accelerate the molecular motion of the “loop” or “tail” segments. Multi-component spectra (Fig. 8a′) which are not remarkable for the homopolymer bulk are observed in the wide temperature range. The immobile labels of the larger splitting than that for the homopolymer bulk, which have strong PMMA–silica interactions are detected even at high temperatures. On the other hand, the extremely smaller splitting for the mobile labels should reflect rapid molecular motion affected by the PEO molecules which are miscible with PMMA at molecular level. Recently, Blum et al. [20] reported the deuterium NMR line shapes of poly(vinyl acetate) adsorbed on silica, which could be divided into rigid or mobile components. They also interpreted the two-component spectra by a distribution of mobilities more heterogeneous than that of the bulk polymer. In the present paper, we studied the ESR spectra of spin-labels of adsorbed PEO and tethered PMMA in the same matrices, silica-t-PMMA, individually to evaluate the rates of motion of the respective polymers. Both polymers have broad distributions of mobilities in comparison with those of the bulk polymers. It seems that the mobile PEO chains accelerate the PMMA chains and the rigid PMMA chains slow down the molecular mobility of the PEO chains. The change of molecular mobility should lead to an increase in breadth of the relaxation phenomena.

References

1. Kobayasi K, Araki K, Imamura Y (1989) Bull Chem Soc Japan 62:3421
2. Kobayasi K, Yajima H, Imamura Y (1980) Bull Chem Soc Japan 63:1813
3. Pan W, Bossmann S, Durning CJ, Turro NJ (1995) Macromolecules 28:7284
4. Ebner S, Keul H, Hocker H (1996) Macromolecules 29:553
5. Shimada S, Sugimoto A, Kawaguchi M (1997) Polymer 38:2251
6. Shimada S, Hane Y, Watanabe T (1997) Polymer 38:4667
7. Kawaguchi M, Sakai A, Takahasi A (1986) Macromolecules 19:2952
8. Kawaguchi M, Hada T, Takahasi A (1989) Macromolecules 22:4045
9. Shimada S, Watanabe T (1998) Polymer 39:1703
10. Shimada S, Watanabe T (1998) Polymer 39:1711
11. Törmälä P, Lindlberg L (1973) Polymer 14:481
12. Shiotani M, Sohma J (1983) Macromolecules 16:1495
13. Tsay F, Gupta A (1987) J Polym Sci Polym Phys Ed 25:855
14. Shimada S, Kashima K (1996) Polymer J 28:690
15. Griffith OH, Dehlinger PJ, Van SP (1974) J Membr Biol 15:159
16. Hommel H, Legrand AP, Ouada HB, Bouchrihat H, Baland H, Papirer E (1992) Polymer 33:181
17. Sakaguchi M, Yamaguchi T, Shimada S, Hori Y (1993) Macromolecules 26:2612
18. Sakaguchi M, Shimada S, Hori Y, Kawaizumi F, Bandow S, Sakai M (1995) Macromolecules 28:8450
19. Shimada S, Suzuki A, Sakaguchi M, Hori Y (1996) Macromolecules 29:973
20. Blum FD, Xu G, Liang M, Wade CG (1996) Macromolecules 29:8740